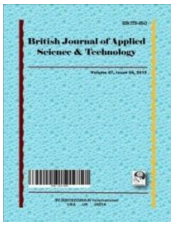

British Journal of Applied Science & Technology
10(6): 1-13, 2015, Article no.BJAST.19147
ISSN: 2231-0843

SCIENCEDOMAIN *international*
www.sciencedomain.org

Useful Working Fluids for Feasible Super Efficient Trilateral Cycles

Ramon Ferreiro Garcia[1*] and Beatriz Ferreiro Sanz[1]

[1]Department of Industrial Engineering, ETSNM, University of A Coruna, Paseo de Ronda 51, 15011, Spain.

Authors' contributions

This work was carried out in collaboration between both authors. Author RFG designed the study, wrote the protocol, the first draft of the manuscript and managed literature searches. Author BFS managed the analyses of the study and literature searches. Both authors read and approved the final manuscript.

Article Information

DOI: 10.9734/BJAST/2015/19147
Editor(s):
(1) Yu Hai-Liang, School of Mechanical, Materials and Mechatronic Engineering, University of Wollongong, Australia.
Reviewers:
(1) Anonymous, Sao Paulo State University, Brazil.
(2) Anonymous, Chungbuk National University, South Korea.
(3) Anonymous, National Cheng Kung University, Taiwan.
Complete Peer review History: http://sciencedomain.org/review-history/10210

Original Research Article

Received 27th May 2015
Accepted 6th July 2015
Published 16th July 2015

ABSTRACT

This work studies feasible trilateral thermal cycles which undergo controlled isothermal expansion path functions. The interest of the study focuses on choosing some working fluids that exhibit operating characteristics such that, first, fulfil the necessary conditions to yield high thermal efficiency in the supercritical region slightly above the critical point, and second, the critical point of each selected working fluid is located within the range of medium and low temperatures. The relevance of the studied working fluids resides in that the trilateral cycle performance can be increased by using the ability of the selected working fluids to exhibiting very high thermal efficiency when operating within the vicinity of its critical point. Thus, on the basis of thermo physical characteristics such the critical temperature, pressure and maximum allowable operating temperature, working fluids have been selected.

The analysis of the trilateral cycle undergoing the transformation of heat into mechanical work on the basis of an isothermal expansion for every selected working fluid has been carried out. The achieved results reveal that almost all candidate working fluids analysed provides high thermal efficiency when operating in the vicinity of the critical point, considering the two best fluids, water for medium top temperatures, and carbon dioxide for low temperatures.

**Corresponding author: E-mail: ferreiro@udc.es;*

Keywords: Carnot factor; low isobaric slope; isothermal expansion; thermal efficiency; trilateral cycle.

NOMENCLATURES

η	*thermal efficiency*
R	*perfect gases constant (kJ/kg-K)*
p	*pressure (bar)*
p_c	*critical pressure (bar)*
q_i	*total specific input heat (kJ/kg)*
q_o	*specific rejected heat (kJ/kg)*
q_v	*isochoric input heat (kJ/kg)*
q_T	*isothermal input heat (kJ/kg)*
q_p	*isobaric rejected heat (kJ/kg)*
s	*specific entropy (kJ/kg-K)*
T	*temperature (K)*
T_c	*critical temperature (K)*
T_{max}	*max. allowable temp. (K)*
u	*internal energy (kJ/kg)*
X_1	*Initial cylinder volume (m)*
X	*fraction of the piston stroke (m)*
W	*specific work (isothermal TC) (kJ/kg)*

ACRONYMS

CF	*Carnot factor*
TC	*Trilateral thermal cycle*

1. INTRODUCTION

During the last decade, growing interest has been observed in utilizing low and medium temperature heat sources, mainly due to its availability from oceans, solar, geothermal and industrial residual heat sources. In this way recently TCs (trilateral cycles) [1-3] are being implemented. Thus, for example, the TC performance has been researched for ammonia-water as working fluid in [2] and ORCs and TCs have been thermodynamically compared in [3]. The author presents a comparison of optimized systems with trilateral cycles with water as working fluid and optimized organic Rankine cycles, where the optimization criterion is the exergy efficiency for power production being the ratio of the net power output to the incoming exergy flow of the heat carrier. The author claims that the exergy efficiency for power production is larger by 14% - 29% for the trilateral cycle than for the ORC.

Whilst ORC and Kalina cycles are used already in existing power plants, the TC, although theoretically mature, it is still under technical development [1]. The components to implement a conventional TC are similar to those in the ORC system except that the working fluid at the entrance of the TC expander (turbine) is a saturated liquid. AS consequence, the state of the working fluid at the expander exit is a two-phase mixture. As the thermodynamic mean temperature at which heat is received is comparatively lower for the TC, the thermal efficiency for this cycle is lower than that for the ORC, for the same temperature limits. The performance of a trilateral cycle has been recently analysed in [4]. Also investigates and compares it with those for the ORC (organic Rankine cycle) and the Kalina cycle, focused on thermodynamics and thermo economics aspects. The results for the TC indicate that an increase in the expander inlet temperature leads to an increase in net output power and a decrease in product cost for this power plant, whereas this is not the case for the ORC system.

Quasi-isothermal compression based reciprocating engines as well as Quasi-isothermal expansion based power cycle engines have been recently developed. In this way, M.W. Coney et al. [5] presented the analysis of a novel concept for a high efficiency reciprocating internal combustion engine called as the isoengine and its cycle, where the maximum net electrical plant efficiency has been predicted to approach about 60% on diesel fuel and 58% on natural gas. They concluded that the key to the high electrical efficiency is the quasi-isothermal compression of the combustion air in cylinders, saving compression work and allowing the recovery of waste heat back into the cycle, mainly from the exhaust gas by means of a recuperator. On the other hand, Opubo N et al. [5], investigated some vapour power cycles for quasi-isothermal expansion instead of adiabatic expansion, taking advantage of the fact that quasi-isothermal expansion has the advantage of bringing the cycle efficiency closer to the ideal Carnot efficiency, with the drawback of requiring heat to be transferred to the working fluid as it expands. The authors claimed that the comparison the specific work output to more standard Stirling engines using gas is higher.

The research effort in this work is focused on trilateral thermal cycles operating under quasi-isothermal expansion instead of adiabatic expansion. Throughout this contribution it will be shown that for low relative operating temperatures the thermal efficiency exceeds the Carnot factor, which makes this thermal cycle

very suitable for exploiting the heat to power conversion cycles with low grade residual heat.

However, in the present work the closed isothermal path functions carried out in the TCs, are appropriated to operate at relative low temperatures, being based on a completely different thermal cycle concept in comparison with the conventional Carnot based thermal cycles, not only structurally but also in terms of CF (Carnot factor) constraints, which can be surpassed in some particular operating conditions [6-7].

Thus, the objective of the study is to efficiently convert low temperature heat mainly from ocean thermal, solar thermal and low grade heat from industrial residual power sources by means of the proposed TCs into electric energy. As it has been indicated, the proposed conversion method is based on a different thermodynamic cycle: a non condensing mode closed processes based TC without regeneration. With this contribution, most of the low grade rejected heat may be converted into mechanical work with acceptable thermal efficiency by applying a TC whose thermal efficiency is not restricted by the CF such as mentioned in [7-9].

2. ANALYSIS OF THE TC UNDERGOING AN ISOTHERMAL EXPANSION

In order to analyse the Isothermal ideal cases, let's consider the displacement of the piston under different path functions as shown in Fig. 1, for the following processes denoted as- Isothermal process (constant temperature) Fig. 1, depicts the mechanical work performed under isothermal thermodynamic transformations when evolving from the state point i to the state point i+1, denoted as the state point 1 and state point 2 respectively.

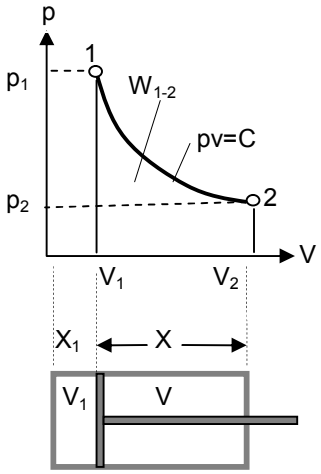

Fig. 1. Mechanical work performed undergoing an isothermal path function

2.1 The Background of the Work Performed under an Isothermal Path Function

According to the scheme depicted in Fig. 1, follows that the mechanical work performed by a piston along its full stroke can be described by means of a general expression as

$$W_{1-2} = \int_{V_1}^{V_2} p \cdot dV \tag{1}$$

Furthermore, considering a closed process undergoing an isothermal transformation, it follows that

$$p \cdot V = p_1 \cdot V_1 = p_2 \cdot V_2 \rightarrow \frac{V_1}{V_2} = \frac{p_2}{p_1} \rightarrow p = \frac{p_1 \cdot V_1}{V} = \frac{R \cdot T_1}{V} \tag{2}$$

therefore, the mechanical work delivered under an isothermal transformation is

$$W_{1-2} = p_1 \cdot V_1 \int_{V_1}^{V_2} \frac{dV}{V} = p_1 \cdot V_1 \cdot Ln\frac{V_2}{V_1} = p_1 \cdot V_1 \cdot \ln\frac{p_1}{p_2} = R \cdot T_1 \cdot Ln\frac{p_1}{p_2} \tag{3}$$

The mechanical work described by Eq. (3) is realisable under the condition that the load (motion resistance) obeys the profile defined by Eq. (2).

2.2 The Proposed TC Undergoing Isochoric Heat Absorption, Isotherm Expansion and Isobaric Heat Rejection Based Path Functions

The proposed TC obeys the processes included between the state points depicted in Figs. 2(a) and 2(b). In this way, Fig. 2(a) shows the T-s diagram, Fig. 2(b) shows the p-V diagram and Fig. 2 (c)

shows the path functions carried out undergoing a closed process based transformation for converting heat into mechanical work.

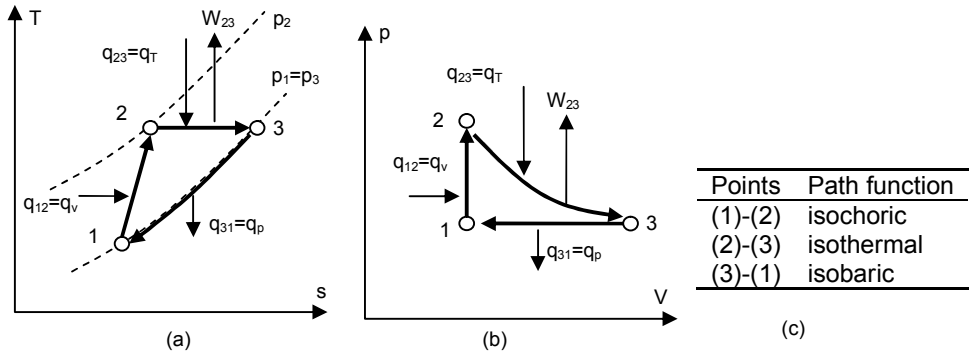

Fig. 2. The T-s and p-V diagrams of the TC undergoing a TC isothermal expansion for converting heat into mechanical work

According to the information provided by the Table 1 and Fig. 2, the transformations associated to each path function of the TC are summarised as follows:

Leg (1)-(2):

Correspond to a closed isochoric heating process. The amount of heat added from an external heat source at constant volume q_v is

$$W_{12} = 0, \quad q_{12} = u_2 - u_1 = Cv \cdot (T_2 - T_1) = q_v \tag{4}$$

Leg (2)-(3): º

Correspond, to a closed isothermal heating process. Consequently the internal energy remains constant so that the total heat added q_T is converted into mechanical works since ideally there are not internal energy changes, and consequently,

$$u_{23} = 0, \text{ and } q_T = W_{23} \tag{5}$$

Since $\frac{p_2}{p_1} = \frac{V_3}{V_1} = \frac{X_1 + X_3}{X_1} = 1 + \frac{X_3}{X_1}$

follows that

$$q_{23} = W_{23} = p_2 \cdot v_2 \cdot Ln(\frac{p_2}{p_1}) = R \cdot T_2 \cdot Ln(\frac{p_2}{p_1}) \tag{6}$$

which can be also expressed as function of the piston location (X) along the cylinder stroke according to the expression (7)

$$q_{23} = W_{23} = p_2 \cdot v_2 \cdot Ln(\frac{V_3}{V_1}) = R \cdot T_2 \cdot Ln\left[1 + \frac{X_3}{X_1}\right] \tag{7}$$

Leg (3)-(1):

Correspond to a closed isobaric process in which the working fluid is cooled. There is not mechanical work so that the rejected heat is coming from the internal energy according to the function

$$W_{31} = 0, \quad q_{31} = u_3 - u_1 = Cv \cdot (T_2 - T_1) = Cv \cdot (T_3 - T_1) = q_p = q_o \tag{8}$$

According to the expressions (7) - (9), the thermal efficiency of the TC undergoing a closed isothermal expansion is given as

$$\eta = 1 - \frac{q_o}{q_i} = 1 - \frac{q_{31}}{q_{12} + q_{23}} = 1 - \frac{q_{31}}{q_{13}} = \frac{W_{23}}{q_{13}} \tag{9}$$

Therefore the thermal efficiency of an isothermal expansion based TC can be expressed analytically, as

$$\eta = \frac{W_{23}}{q_{13}} = \frac{W_{23}}{(u_2 - u_1) + W_{23}} == \frac{R \cdot T_2 \cdot Ln\left[1 + \frac{X_3}{X_1}\right]}{(u_2 - u_1) + R \cdot T_2 \cdot Ln\left[1 + \frac{X_3}{X_1}\right]} \tag{10}$$

Since ideally the heat added to the transformation (2)-(3) is converted into mechanical work, the thermal efficiency defined in (10) exhibits a strong dependence on the difference of temperatures (T_2-T_1). Apparently, the thermal efficiency tends to the unity when such temperature difference tends to zero. However, real gases behaviour differs from this model.

Furthermore, even that

$$q_v = q_{12} = u_2 - u_1 = Cv \cdot (T_2 - T_1),$$

$$q_o = q_p = q_{31} = u_3 - u_1 = Cv \cdot (T_3 - T_1),$$

and

$$T_3 = T_2,$$

follows that

$$q_v = q_o \tag{11}$$

and

$$q_i = q_v + q_T = q_v + W$$

Consequently, since

$$\eta = \frac{q_i - q_o}{q_i} = \frac{q_v + W - q_o}{q_i} = \frac{q_v + W - q_v}{q_i} = \frac{W}{q_v + W}$$

follows that

$$\lim_{q_v \to 0}(\eta) = \lim_{q_v \to 0} \frac{W}{q_v + W} = 1 \tag{12}$$

Eq. (12), as well as Eq. (10) suggests us that considering a reversible TC, when T_2 approaches T_1, or q_v approaches zero, the thermal efficiency tends to the unity. However,

since $q_v > 0$, then, $\eta < 1$, as stated by the second law.

3. A CASE STUDY

This section deals with the exploration and analysis of a case study in which a TC composed by closed systems based transformations is applied on the conversion of heat to mechanical work undergoing an isothermal expansion based path function to change from state point 2 to state point 3.

3.1 The Structure of the TC Undergoing Isothermal Expansion to Convert Heat into Mechanical Work

The Fig. 3 represents a closed processes based TC implemented by means of a single effect cylinder in which Fig. 3(a) shows the single effect cylinder, Fig. 3(b), shows the sequence of processes carried out to complete the cycle, and Fig. 3(c) shows the corresponding p-V and T-s diagrams assuming isothermal expansion.

The TC shown In Fig. 3 consists of a single effect cylinder-actuator which could operate optionally with several working fluids including but not limited to carbon dioxide or water, as well as other gases that remain at gaseous state at ambient temperature. The cylinder is equipped with heating and cooling facilities. The piston road could drive a reciprocating hydraulic pump for instance or any other load type. Although not analysed in this work and consequently not represented in Fig 3, the possibility of regenerating some residual heat exits due to the fact that the residual heat corresponding to the working fluid temperature at the end of the expansion could be reused. Consequently, the possibility of increasing the thermal efficiency by regeneration is a real fact. The thermal cycle depicted in Fig 3 can be easily understood by observing the associated table as well as the p-V and T-s diagrams shown in Fig. 3 (c).

In the associated table of Fig. 3 (b) the ports X and Y means the heater and cooler heat flows. Thus X = 1 means that heat is entering to the cylinder, while Y = 1 means that heat is being rejected from the cylinder to the environment. X=Y=0 indicates no heat transfer activity.

Considering the active chamber of the cylinder depicted in Fig. 3 (a), and the T-s diagram shown also in the Fig. 3 (c), the TC starts in the state point 1, with a working fluid under a pressure, temperature, specific volume and entropy corresponding to the state point 1. After some heat has been added (q_{12}) at constant volume (isochoric process), the pressure, temperature and entropy corresponds to the state point 2. The transformation 2-3 undergoes constant temperature, so that the heat added (q_{22}) is converted theoretically into mechanical work at constant temperature (isothermal process), since the internal energy will remain constant along the transformation 2-3. The last transformation corresponds to the heat rejection q_{31} towards the heat sink which might be the environment.

As pressure decreases as consequence of the isothermal expansion, the mechanical load reacting against the piston rod is balanced to satisfy the condition of constant internal energy along the piston stroke until the bottom dead centre.

After expansion has finished in the state point (3), the piston initiates the way back towards the point (1) (the top dead centre) at constant pressure, while is being cooled, so that the cycle is completed.

3.2 The Selected Working Fluids

The working fluids shown in Table 1 under study were selected after a search process from a vast amount of available fluids according to reference [10] such as to satisfy certain conditions in the supercritical region above the critical point. Furthermore, the required conditions are defined for a region located at the vicinity of the critical point as:

The isobaric slope shown in Fig. 4 defined according to the T-s diagram,

$$\frac{dT}{ds} \to 0, \tag{13}$$

the Isobaric slope shown in Fig. 5 defined according to the T-h diagram,

$$\frac{dT}{dh} \to 0, \tag{14}$$

and the isothermal slope shown in the Fig. 6 defined according to the p-h diagram

$$-\frac{dp}{dh} \to 0 \tag{15}$$

Such characteristic, shown in Figs. 4, 5 and 6 for the case of water is used to define the region of maximum thermal efficiency. The consequence of this characteristic is summarised as follows: That is, the selected working fluids exhibit the highest thermal efficiency when operating within a region above its critical point.

Table 1. The selected working fluids, showing the critical conditions and the maximum allowable operating temperature from [10]

WF	T_c (K)	p_c (bar)	Tmax (K)
Ethylene	282.35	50.42	450
Xenon	289.73	58.42	750
CO_2	304.01	73.77	2000
Ethane	305.32	48.72	675
R41	317.28	58.97	425
R218	345.02	26.40	440
R143a	345.86	37.61	650
R32	351.26	57.82	435
Propylene	364.21	45.55	575
Propane	369.89	42.51	625
R134a	374.21	40.59	455
RC318	388.38	27.77	623
Ammonia	405.40	113.33	700
Methanol	512.60	81.03	620
Ethanol	513.90	61.48	650
Water	647.10	220.64	2000

Table 2. Potential working fluids, showing the critical conditions and the maximum allowable operating temperature from [10]

WF	T_c (K)	p_c (bar)	Tmax (K)
Toluene	591,75	41,26	700
Hexane	507,82	30,34	600
Heptane	540,13	27,36	600
Decane	617,70	21,03	675
Cyclo hexane	553,64	40,75	700
Acetone	508,10	47,00	550

3.3 Modelling the TC

The TC modelling task has been carried out with data extracted from [10] (REFPROP) and the tool Engineering Equation Solver (EES). The REFPROP consists of an up-to date data base used for property calculations and is available in commercial software packages whose library makes use of Helmholtz fundamental equation correlations to determine fluid properties from the highest-accuracy published data available in literature. Furthermore, the database can be linked with software based tools such Visual Basic, Fortran, C, and even spread sheets to help the automation of data processing. In the proposed case study the data necessary to carry out the performance analysis is presented in Table A1 of the appendix A.

For the analysis of the cycle with the considered working fluids exhibiting the characteristics shown in Table 1, the necessary tests has been carried out to study the cycles performance and behaviour.

4. MAIN RESULTS OF THE ANALYSED CASE STUDY

The results of the study achieved using the EES yield the values of Table 3 using the data shown in Table A1 of the appendix A. The data used in the case study for the study of the potential working fluids is taken from reference [10]. Cycle computation is referred to the T-s diagram of Fig. 7 for a non-regenerative TC. The values of the state variables corresponding to each state point for all considered working fluids are shown in the Table A1 of the appendix A, where for every working fluid a set of top and bottom temperatures has been considered, as shown in Table 3. Table 3 shows for every selected working fluid

Critical temperature T_c (K),
Bottoming TC temperature T_1 (K),
Topping TC temperature T_2 (K),
Critical TC pressure p_c (bar),
Bottoming TC pressure p_1 (bar),
Topping TC pressure p_2 (bar),
Thermal efficiency η (%)
Carnot factor CF (%), and
Specific work W (kJ/kg)

In Table 3, the WFs are represented by its critical temperature in ascendant order. The bottoming temperature T_1(K) is chosen bellow ten degrees from the critical temperature. The topping temperature is chosen between 20-30 degrees above the bottoming temperature. The bottoming pressure is chosen between 2-4 bar above the critical pressure, and the topping pressure p2 (bar), is associated with the topping temperature. The topping TC temperature has been chosen to fulfil the requirement of high thermal efficiency in the region above the critical point. Since the ratio of the bottoming to the topping temperatures is low, the corresponding CF is also low. However since the thermal efficiency of the TC is independent of the CF, the thermal efficiency is significantly high.

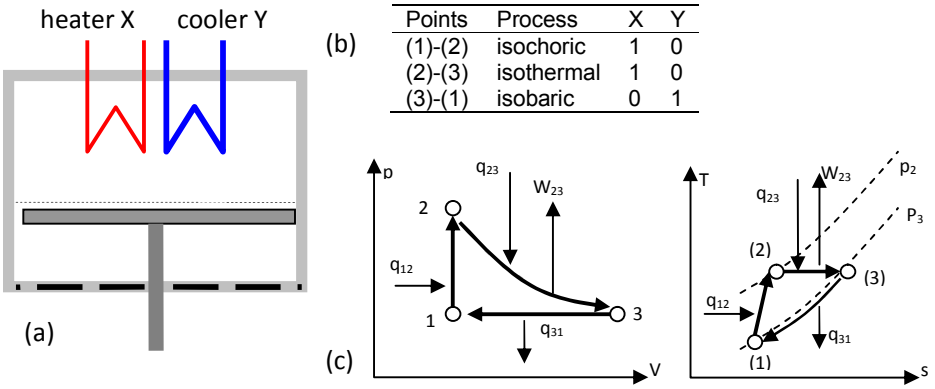

Points	Process	X	Y
(1)-(2)	isochoric	1	0
(2)-(3)	isothermal	1	0
(3)-(1)	isobaric	0	1

Fig. 3. A closed processes based TC implemented with a single effect cylinder. (a), single effect cylinder. (b), processes sequence. (c), the p-V and T-s diagrams

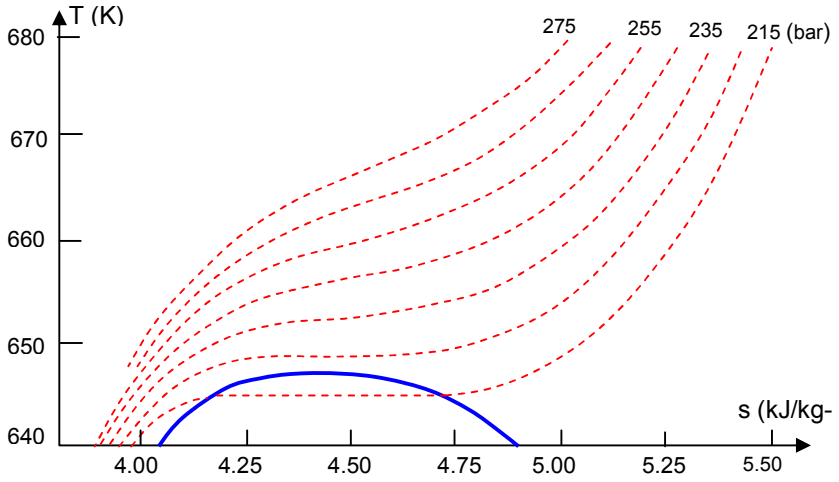

Fig. 4. T-s diagram for H_2O as working fluid, operating in the vicinity of the critical conditions, for which the slope of the isobars (dT/ds) approaches zero

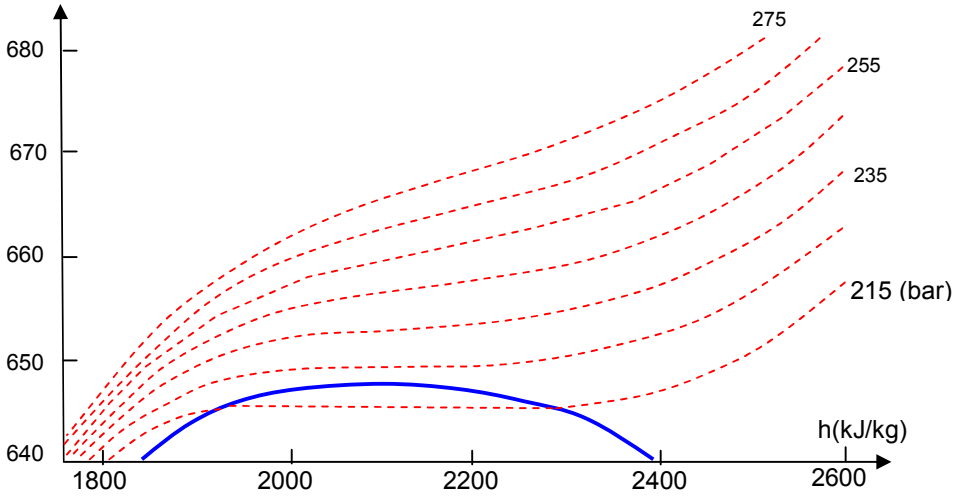

Fig. 5. T-h diagram for H_2O as working fluid, operating in the vicinity of the critical conditions, for which the slope of the isobars (dT/dh) approaches zero

In order to facilitate the analysis of the results to extract useful conclusions, Table 4, shows the studied working fluids ordered in descendent order by thermal efficiency, specific work, topping temperature and topping pressure. This table is useful to highlight the working fluid that satisfies the desired conditions. Thus, focusing on the thermal efficiency follows that the best WF is water, whose thermal efficiency approaches 87%, and if focusing on the specific work, follows that the specific work approaches 2180 kJ/kg. The available topping temperatures associated with the residual heat source is also important to select the appropriated WF. Thus, water requires a power source capable to heat the working fluid till 675 K, which undergoes a topping pressure of 273 bar. Consequently, the same considerations must be taken into account for the rest of the studied fluids.

Table 3. The performance of a TC operating with the studied working fluids presented in ascendant order by its critical temperature

WF	T_c (K)	T_1(K)	T_2(K)	p_c (bar)	p_1 bar)	p_2 (bar)	η(%)	CF(%)	W(kJ/kg)c
Ethylene	282.35	286	310	50.42	53	72	56	7.74	350
Xenon	289.73	300	325	58.42	60	73	75	7.69	25
CO_2	304.01	300	325	73.77	75	174	76	7.69	474
Ethane	305.32	310	340	48.72	52	74	77	8.82	356
R41	317.28	321	345	58.97	62	89	84	6.96	482
R218	345.02	350	375	26.4	30	49	41	6.67	146
R143a	345.86	350	375	37.61	41	62	82	6.67	327
R32	351.26	355	380	57.82	62	90	85	6.58	495
Propylene	364.21	368	415	45.55	49	95	77	11.33	630
Propane	369.89	375	400	42.51	45	83	75	6.25	300
R134a	374.21	378	405	40.59	44	69	82	6.67	326
R318	388.38	393	420	27.77	32	55	74	6.43	154
Ammonia	405.4	410	440	113.33	115	160	76	8.89	740
Methanol	512.6	520	540	81.035	85	101	79	3.70	602
Ethanol	513.9	520	540	61.48	64	75	77	3.70	359
Water	647.1	650	675	220.64	225	273	87	3.70	2180

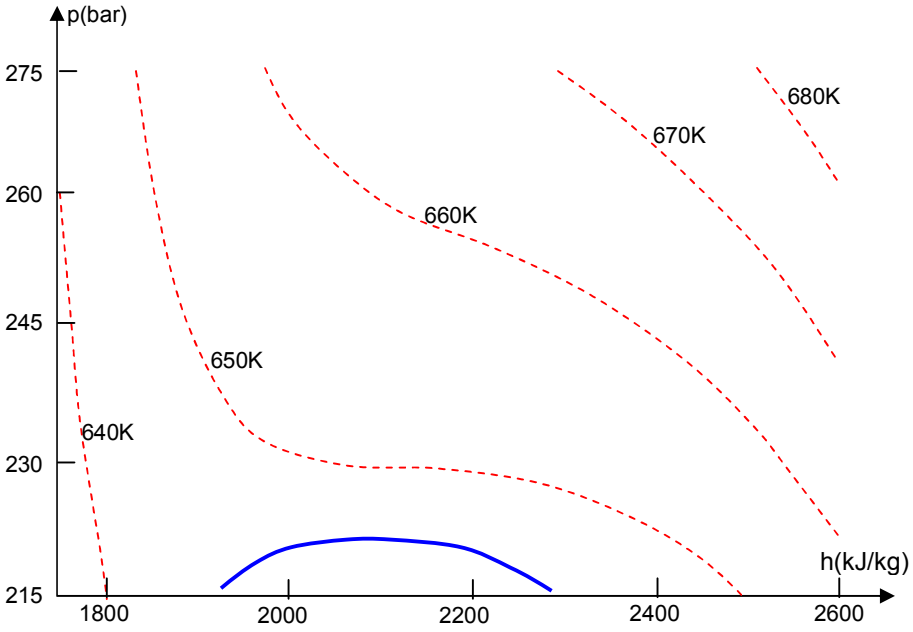

Fig. 6. p-h diagram for H_2O as working fluid, operating in the vicinity of the critical conditions, for which the slope of the isothermals (-dp/dh) approaches zero

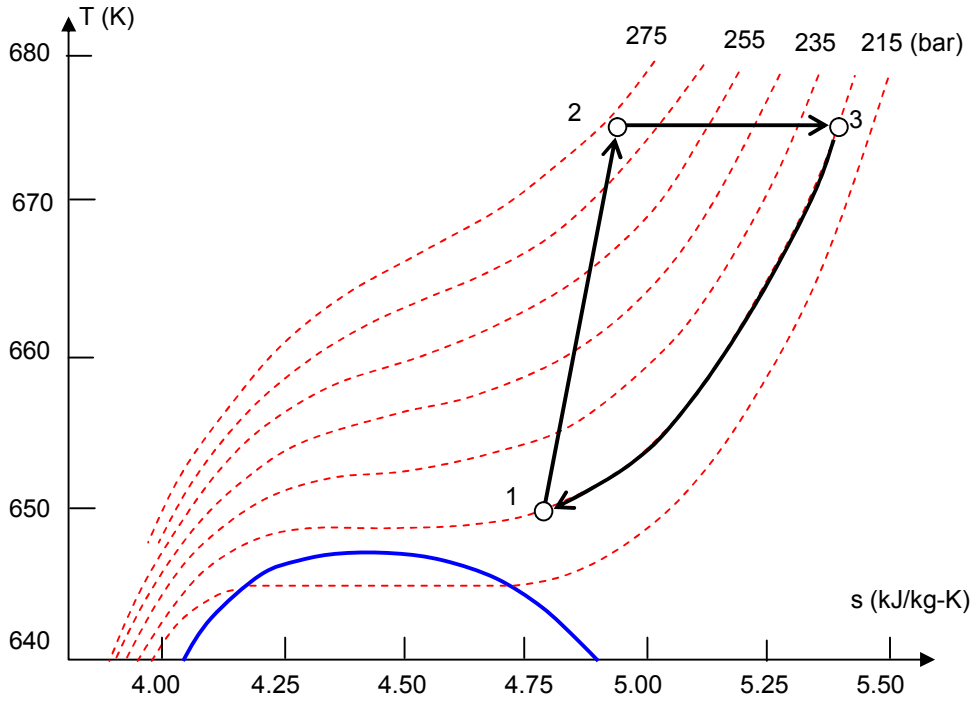

Fig. 7. The layout of the TC for water as working fluid, operating in a region above the critical point

Table 4. The studied working fluids ordered in descendent order by thermal efficiency, specific work, top temperature and top pressure

WF	η(%)	WF	W (kJ/kg)	WF	T_2 (K)	WF	p_2 (bar)
Water	87	Water	2180	Water	675	Water	273
R32	85	Ammonia	740	Methanol	540	CO_2	174
R41	84	Propylene	630	Ethanol	540	Ammonia	160
R143a	82	Methanol	602	Ammonia	440	Methanol	101
R134a	82	R32	495	R318	420	Propylene	95
Methanol	79	R41	482	Propylene	415	R32	90
Ethane	77	CO_2	474	R134a	405	R41	89
Propylene	77	Ethanol	359	Propane	400	Propane	83
Ethanol	77	Ethane	356	R32	380	Ethanol	75
CO_2	76	Ethylene	350	R218	375	Ethane	74
Ammonia	76	R143a	327	R143a	375	Xenon	73
Xenon	75	R134a	326	R41	345	Ethylene	72
Propane	75	Propane	300	Ethane	340	R134a	69
R318	74	R318	154	Xenon	325	R143a	62
Ethylene	56	R218	146	CO_2	325	R318	55
R218	41	Xenon	25	Ethylene	310	R218	49

5. CONCLUSION

Trilateral thermal cycles operating with some working fluids characterised by the process of conversion heat into mechanical work undergoing controlled isothermal expansion path functions in a region above the critical point, have been studied. By means of the study, It has been shown that trilateral cycles performance can be improved by using the ability of the selected working fluids to yield high thermal

efficiency when operating within a supercritical region above the critical point.

The objective of the study consisted of highlighting the operating characteristics of potential working fluids operating on a trilateral thermal cycle undergoing isothermal expansion path functions.

As result of the study carried out, some data concerning useful criteria to select the appropriate working fluid as function of the feasible operating conditions, is highlighted. Therefore, taking as performance criteria the thermal efficiency, follows that the top ten working fluids are: Water, R32, R41, R143a, R134a, Methanol, Ethane, Propylene, Ethanol and CO_2, while the thermal efficiency is within the range of 76% for CO_2 to 87% for water.

However, taking as performance criteria the specific work, follows that the top ten working fluids are: Water, Ammonia, Propylene, Methanol, R32, R41, CO_2, Ethanol, Ethane and Ethylene, while the specific work is within the range of 350 kJ/kg for Ethylene to 2180 kJ/kg for water.

According to the obtained results it follows that water meets most of the criteria of selection, since it provides high efficiency and specific work, despite need a heat source whose upper temperature is above 675 K.

From the analysis of the case study it can be highlighted also the independence of the thermal efficiency with respect to the CF, as well as the high thermal efficiency at low top temperatures with respect to CF.

COMPETING INTERESTS

Authors have declared that no competing interests exist.

REFERENCES

1. Smith IK. Development of the trilateral flash cycle system: Fundamental considerations. J Power Energy Proc IMechE. 1993;207:179-194.
2. Zamfirescu C, Dincer I. Thermodynamic analysis of a novel ammonia-water trilateral Rankine cycle. Thermochim Acta. 2008;447:7-15.
3. Fischer J. Comparison of trilateral cycles and organic Rankine cycles. Energy. 2011; 36:6208-6219.
4. Yari M, Mehr AS, Zare V,. Mahmoudi SMS, Rosen MA. Exergoeconomic comparison of TC (trilateral Rankine cycle), ORC (organic Rankine cycle) and Kalina cycle using a low grade heat source. Energy. 2015;83:712-722. Available:http://dx.doi.org/10.1016/j.energy.2015.02.080
5. Coney MW, Linnemann C, Abdallah HS. A thermodynamic analysis of a novel high efficiency reciprocating internal combustion engine - the isoengine. Energy. 2004;29: 2585-2600.
6. Opubo N. Igobo, Philip A. Davies. Review of low-temperature vapour power cycle engines with quasi-isothermal expansion. Energy. 2014;70:22-34.
7. Xiaohui S, Yonggao Y, Xiaosong Z. Thermodynamic analysis of a novel energy-efficient refrigeration system subcooled by liquid desiccant dehumidification and evaporation. Energy Conversion and Management. 2014;78: 286-296.
8. Ramon Ferreiro Garcia, Beatriz Ferreiro Sanz. Isothermal and adiabatic expansion based trilateral cycles. British Journal of Applied Science & Technology. 2015; 4(26):3840-3855.
9. Ramon Ferreiro Garcia, Beatriz Ferreiro Sanz. The behaviour of some working fluids applied on the trilateral cycles with isothermal controlled expansion. British Journal of Applied Science & Technology. 2015; 9(5):450-463.
10. Lemmon EW, Huber ML, McLinden MO. NIST reference fluid thermodynamic and transport properties - REFPROP version 8.0, User's Guide, NIST 2007, Boulder, Colorado.

APPENDIX A

The Data for the Case study

Table A1. The state variables of the TC state points for each working fluid using data from [10]

Point	T(K)	U(kJ/kg)	S(kJ/kg-K)	P(bar)	V(m³/kg)	Cv(kJ/kg-K)	Cp(kJ/kg-K)
				Ethylene			
1	286	242.50	1.8661	53.00	0.0065016	1.7941	17.5020
2	310	463.80	1.9982	71.55	0.0065016	1.5680	5.3269
3	310	514.35	2.2634	53.00	0.0116540	1.4546	2.8955
				Xenon			
1	286	79.46	0.34864	60.00	0.0017389	0.15116	0.80284
2	310	82.93	0.35977	73.32	0.0017389	0.13007	0.51235
3	310	87.82	0.38872	60.00	0.0024211	0.12078	0.36145
				Carbon dioxide			
1	300	263.16	1.2389	75.0	0.0013626	1.01150	4.5507
2	325	287.15	1.3157	173.6	0.0013626	0.92975	2.6663
3	325	409.93	1.8115	75.0	0.0052833	0.87759	2.0648
				Ethane			
1	310	465.17	1.8807	52	0.0065865	2.1002	17.5510
2	340	523.82	2.0613	73.64	0.0065865	1.9091	5.1564
3	340	579.95	2.3332	52	0.0124730	1.8038	3.0446
				R41			
1	321	422.37	1.7943	62	0.0045553	1.5872	17.0970
2	345	457.76	1.9007	88.97	0.0045553	1.3931	5.2600
3	345	513.10	2.1452	62	0.0085816	1.2491	2.7047
				R218			
1	350	299.61	1.3229	30.00	0.0013716	0.94369	4.7850
2	375	323.00	1.3874	48.64	0.0013716	0.93219	1.7401
3	375	507.00	1.4682	30.00	0.0035110	0.91030	1.2430
				R143a			
1	350	355.17	1.5047	41.000	0.0023015	1.2904	18.1590
2	375	385.41	1.5882	61.897	0.0023015	1.1631	3.2825
3	375	427.15	1.7446	41.000	0.0056976	1.0969	1.7566
				R32			
1	355	416.66	1.6996	62.00	0.0026641	1.3698	30.4840
2	380	447.23	1.7829	89.63	0.0026641	1.1357	4.6686
3	380	507.00	2.0073	62.00	0.0061036	1.0230	2.1137
				Propylene			
1	368	509.31	1.9755	49.00	0.0039899	2.2669	36.071
2	415	602.66	2.2144	95.31	0.0039899	1.9668	4.2474
3	415	699.75	2.5764	49.00	0.0120670	1.8900	2.6590
				Propane			
1	375	584.80	2.2043	45.00	0.0063476	2.2841	12.7760
2	400	640.00	2.3468	58.15	0.0063476	2.1835	5.1099
3	400	681.97	2.5091	45.00	0.0108360	2.0958	3.2220
				R134a			
1	378	382.88	1.5639	44.0	0.0018325	1.1970	15.9300
2	405	413.58	1.6423	69.2	0.0018325	1.1056	2.8831
3	405	456.39	1.7881	44.0	0.0048227	1.0462	1.6087
				RC318			
1	393	350.14	1.4553	32.0	0.0012416	0.98413	3.2729
2	420	376.65	1.5184	55.2	0.0012416	0.98218	1.6558
3	420	404.27	1.6048	32.0	0.0034229	0.96473	1.3079

Ammonia							
1	410	1384.8	4.5376	115.00	0.0075433	2.3343	19.2710
2	450	1504.7	4.8171	159.56	0.0075433	2.7662	7.7850
3	450	1622.3	5.2520	115.00	0.0133260	2.4789	4.7618
Methanol							
1	520	997.5	2.2890	85.00	0.0068431	3.8581	16.8000
2	540	1071.7	2.4292	101.33	0.0068431	3.5848	9.9258
3	540	1150.7	2.6308	85.00	0.010068	3.6308	6.1979
Ethanol							
1	520	1310.5	3.7282	64.00	0.0070698	2.8564	11.4110
2	540	1367.4	3.8356	75.2	0.0070698	2.8338	6.9549
3	540	1416.8	3.9655	64.00	0.010047	2.6683	4.5573
Water							
1	650	2221.6	4.7753	225.0	0.0045813	4.2412	65.2720
2	675	2314.3	4.9154	273.3	0.0045813	3.3843	19.992
3	675	2548.4	5.3885	225.0	0.0080085	2.9018	8.1990

© 2015 Garcia and Sanz; This is an Open Access article distributed under the terms of the Creative Commons Attribution License (http://creativecommons.org/licenses/by/4.0), which permits unrestricted use, distribution, and reproduction in any medium, provided the original work is properly cited.

Peer-review history:
The peer review history for this paper can be accessed here:
http://sciencedomain.org/review-history/10210